SUPPLEMENTAL METHODS

Morphological analysis by scanning electron microscopy (SEM) ---Glutaraldehyde (2%) and paraformaldehyde (2%)-fixed inner ears were microdissected, stepwise dehydrated in ethanol solutions, and eventually freeze-dried in *t*-butyl alcohol. Prepared inner ears were then mounted on aluminum stubs with colloidal silver adhesive and sputter-coated with gold palladium before imaging in a Hitachi S-800s scanning electron microscope.

Endocochlear potential---Endocochlear potentials from WT, *Ednrb(-/-)*-mice and *Ednrb(-/-);DBH-Ednrb*-mice were recorded with a dual electrometer (FD-223; WPI) against an Ag/AgCl reference inserted under the skin, and they were monitored with a Mac Lab 8s (ADInstruments) (1).

TUNEL staining---Terminal deoxynucleotidyl transferase-mediated dUTP nick-end labeling (TUNEL) with 4% paraformaldehyde fixative solution was performed following the instructions of the manufacturer (Chemicon) with a previously reported positive control of hair bulge cells (2).

REFERENCES

1. Komune, S., Nakagawa, T., Hisashi, K., Kimitsuki, T., and Uemura, T. (1993) *Hear. Res.* **70,** 197-204
2. Ito, M., Kizawa, K., Toyoda, M., and Morohashi, M. (2002) *J. Invest. Dermatol.* **119,** 1310-1316
3. Nishimura, E. K., Jordan, S. A., Oshima, H., Yoshida, H., Osawa, M., Moriyama, M., Jackson, I. J., Barrandonk, Y., Miyachi, Y., and Nishikawa, S.-I. (2002) *Nature* **416,** 854-860
4. Amiel, J., Attié, T., Jan, D., Pelet, A., Edery, P., Bidaud, C., Lacombe, D., Tam, P., Simeoni, J., Flori, E., Nihoul-Fékété, C., Munnich, A., and Lyonnet, S. (1996) *Hum. Mol. Genet.* **5,** 355-357
5. Svensson, P.-J., Anvret, M., Molander, M.-L., and Nordenskjöld, A. (1998) *Hum. Genet.* **103,** 145-148
6. Hofstra, R. M., Osinga, J., and Buys, C. H. (1997) *Eur. J. Hum. Genet.* **5,** 180-185
7. Attié, T., Till, M., Pelet, A., Amiel, J., Edery, P., Boutrand, L,, Munnich, A., and Lyonnet, S. (1995) *Hum. Mol. Genet.* **4,** 2407-2409
8. Boardman, J. P., Syrris, P., Holder, S. E., Robertson, N. J., Carter, N., and Lakhoo, K. (2001) *J. Med. Genet.* **38,** 646-647
9. Sangkhathat, S., Chiengkriwate, P., Kusafuka, T., Patrapinyokul, S., and Fukuzawa, M. (2005) *Pediatr. Surg. Int.* **21,** 960-963
10. Gross, A., Kunze, J., Maier, R. F., Stoltenburg-Didinger, G., Grimmer, I., and Obladen, M. (1995) *Am. J. Med. Genet.* **56,** 322-326
11. Verheij, J. B., Kunze, J., Osinga, J., van Essen, A. J., and Hofstra, R. M. W. (2002) *Am. J. Med. Genet.* **108,** 223-225
12. Syrris, P., Carter, N. D., and Patton, M. A. (1999) *Am. J. Med. Genet.* **87,** 69-71
13. Kusafuka, T., Wang, Y., and Puri, P. (1996) *Hum. Mol. Genet.* **5,** 347-349

14. Puffenberger, E. G., Hosoda, K., Washington, S. S., Nakao, K., deWit, D., Yanagisawa, M., and Chakravarti, A. (1994) *Cell* **79,** 1257-1266
15. Auricchio, A., Griseri, P., Carpentieri, M. L., Betsos, N., Staiano, A., Tozzi, A., Priolo, M., Thompson, H., Bocciardi, R., Romeo, G., Ballabio, A., and Ceccherini, I. (1999) *Am. J. Med. Genet.* **64,** 1216-1221
16. Auricchio, A., Casari, G., Staiano, A., and Ballabio, A. (1996) *Hum. Mol. Genet.* **5,** 351-354

SUPPLEMENTAL FIGURE LEGENDS

Fig. S1. Immunohistochemistry of EdnrB in hair cells of WT, *Ednrb(-/-)* and *Ednrb(-/-);DBH-Ednrb*-mice. The organs of Corti from WT (*A*), *Ednrb(-/-)* (*B*) and *Ednrb(-/-); DBH-Ednrb*-mice (*C*) on P19 were immunohistochemically analyzed with anti-Ednrb antibody. No signals were detected at the organ of Corti from *Ednrb(-/-)*, *Ednrb(-/-); DBH-Ednrb* and littermate WT-mice on P19 (*A*-*C*). Scale bars: 50 μm.

Fig. S2. Morphological analyses of hair cells from WT, *Ednrb(-/-)* and *Ednrb(-/-);DBH-Ednrb*-mice on P17. Scanning electron microscopy showed no morphological differences in inner hair cells (IHC) and outer hair cells (OHC) at equivalent positions between *Ednrb(-/-)* (*B*), *Ednrb(-/-);DBH-Ednrb* (*C*) and littermate WT-mice (*A*). Magnified figures of IHC and OHC in *A*-*C* are shown in *D*-*F* and in *G*-*I*, respectively. Scale bars: 10 μm (*A*-*C*), 3 μm (*D*-*I*).

Fig. S3. Apoptotic signals in SGNs. *A*-*C,* SGNs from *Ednrb(-/-)* (*B*), *Ednrb(-/-);DBH-Ednrb* (*C*) and littermate WT-mice (*A*) on P19 were stained by the TUNEL method. *D*-*F*, the corresponding views were visualized under a phase contrast microscope. No apoptotic signals were detected at SGNs from *Ednrb(-/-), Ednrb(-/-);DBH-Ednrb* and littermate WT-mice on P19. Scale bars: 10 μm.

Fig. S4. Measurement of endocochlear potentials. Endocochlear potentials from 10-week-old WT (n = 5) and *EdnrB(-/-);DBH-Ednrb*-mice (n = 5) were recorded. **, $P < 0.01$ (Mann-Whitney *U*-test).

Fig. S5. Hair color of WT, *Ednrb(-/-), Ednrb(-/-);DBH-Ednrb*-mice on P28. *A*, WT, *Ednrb(-/-)* and *Ednrb(-/-);DBH-Ednrb*-mice on P28. Coat color is indistinguishable between *Ednrb(-/-)* and *Ednrb(-/-);DBH-Ednrb*-mice. Scale bar: 1 cm. *B*, *Dct*-LacZ staining of the skin (3). LacZ-positive cells in WT-mice indicate melanocytes in the hair follicles (arrows). Follicular melanocytes are absent in *Ednrb(-/-)* and *Ednrb(-/-);DBH-Ednrb*-mice. Scale bar: 100 μm.

Fig. S6. Suprathreshold ABR analysis in *Ednrb(-/-);DBH-Ednrb*-mice and littermate WT-mice on P10, P14 and P19. The amplitude versus sound level relationship (means ± SE) of the 12 kHz wave I obtained during ABR analysis of *Ednrb(-/-);DBH-Ednrb*-mice (red diamonds, $n = 6$) and littermate WT-mice (black squares, $n = 6$) on P10 (*A*), P14 (*B*) and P19 (*C*) was plotted. The slope of amplitude growth was similar in of *Ednrb(-/-);DBH-Ednrb*-mice and WT-mice on P14 and P19.

Fig. S7. Genome structure of Ednrb mutant mice and summary of human *EDNRB* gene mutations. *A,* Schema of genomic structure of wild type (WT), spotting lethal (*sl*), Waardenburg-Shah syndrome IV (*WS-IV*) and *Ednrb(-/-)*-mice [*Ednrb(-/-)*]. *sl* mice have spontaneous deletions of exon 1 and intron 1, while *WS-IV* mice have spontaneous deletions of exon 2 and exon 3. *Ednrb(-/-)*-mice analyzed in this study have a deletion of exon 3. The hearing levels of *Ednrb(-/-)*-mice have not been reported. *B,* Summary of point mutations in

human *EDNRB* gene causing WS or Hirschsprung disease (Hirsch). ABCD: albinism, black locks, cell migration disorder of neurocytes of the gut and deafness. (ter): termination. Human patients with WS caused by point mutations in exon 3 of *EDNRB* have been reported to suffer from deafness (10-12).

Fig. S1

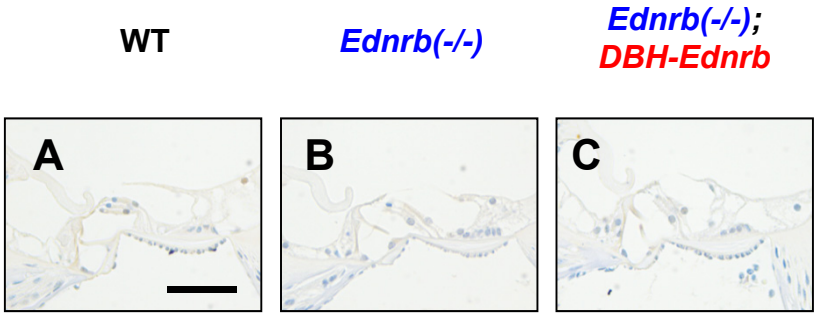

Fig. S2

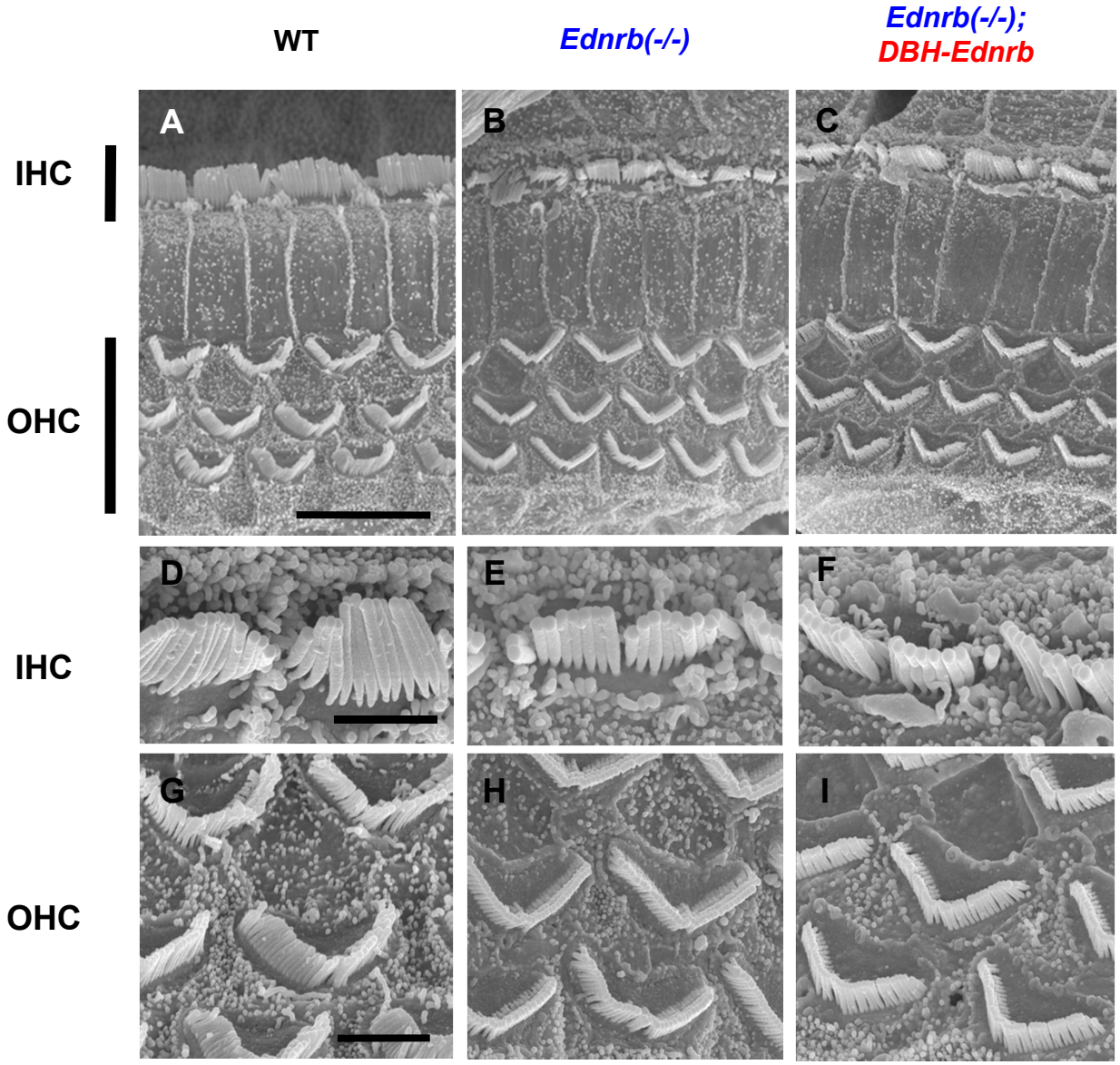

Fig. S3

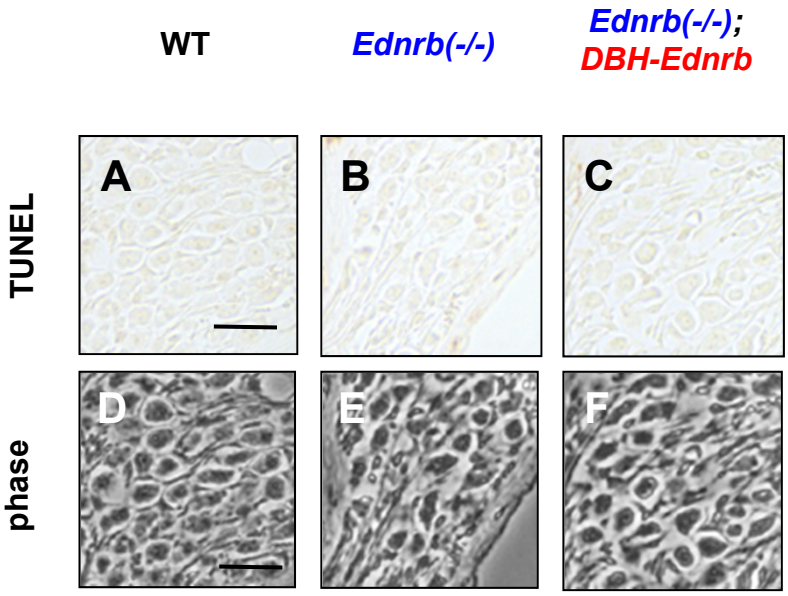

Fig. S4

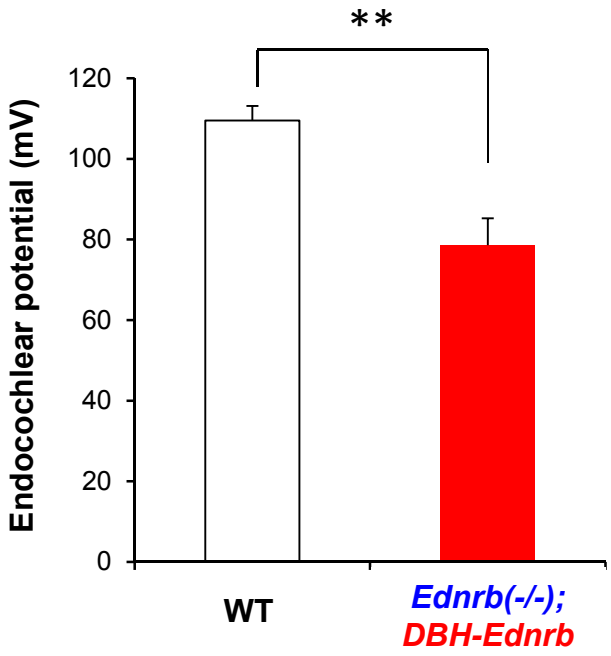
**
120
100
80
60
40
20
0
Endocochlear potential (mV)
WT
Ednrb(-/-);
DBH-Ednrb

Fig. S5

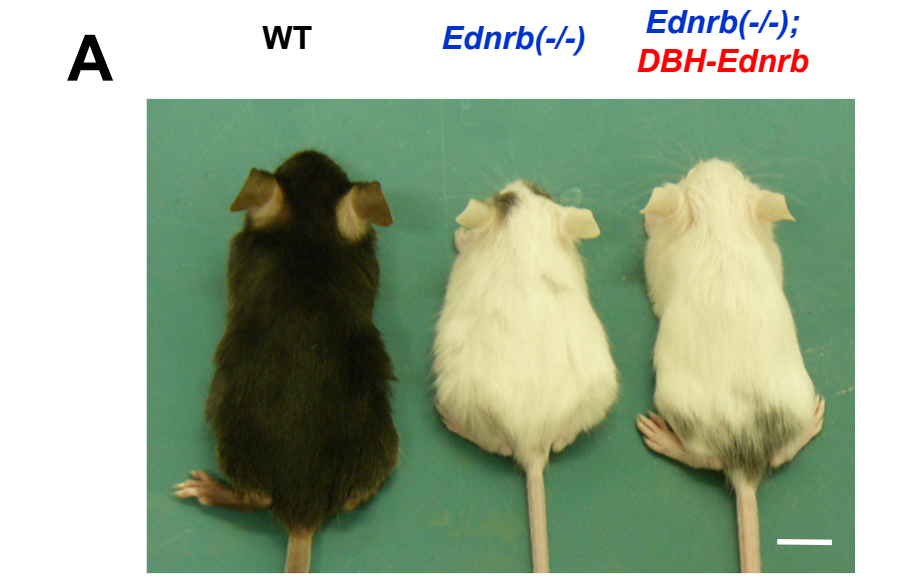

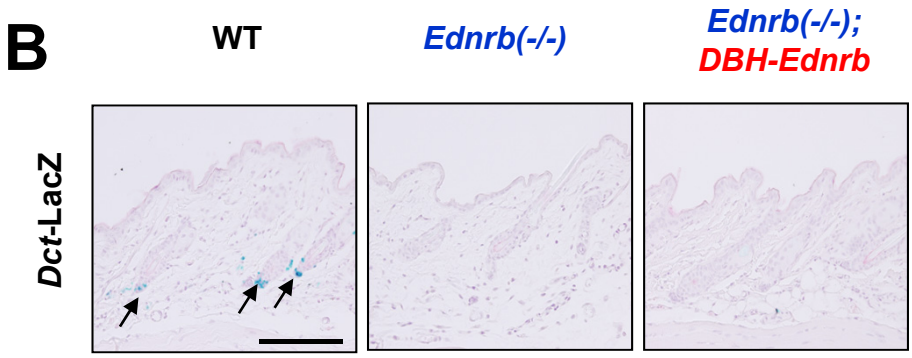

Fig. S6

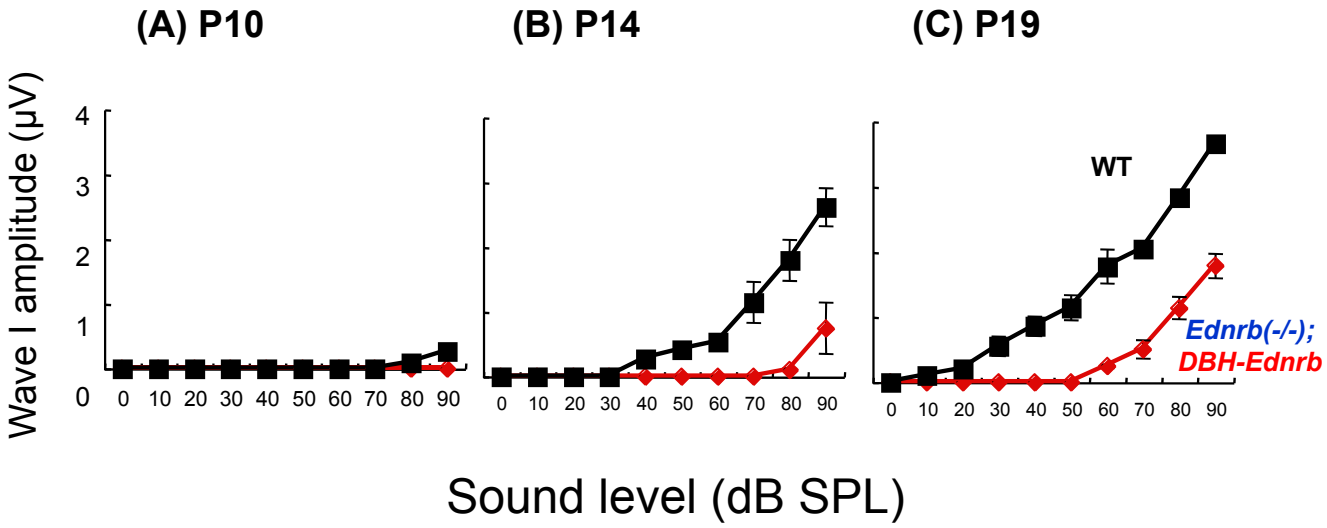
(A) P10
(B) P14
(C) P19
Wave I amplitude (μV)
0
1
2
3
4
0 10 20 30 40 50 60 70 80 90
WT
Ednrb(-/-);
DBH-Ednrb
Sound level (dB SPL)

Fig. S7

A

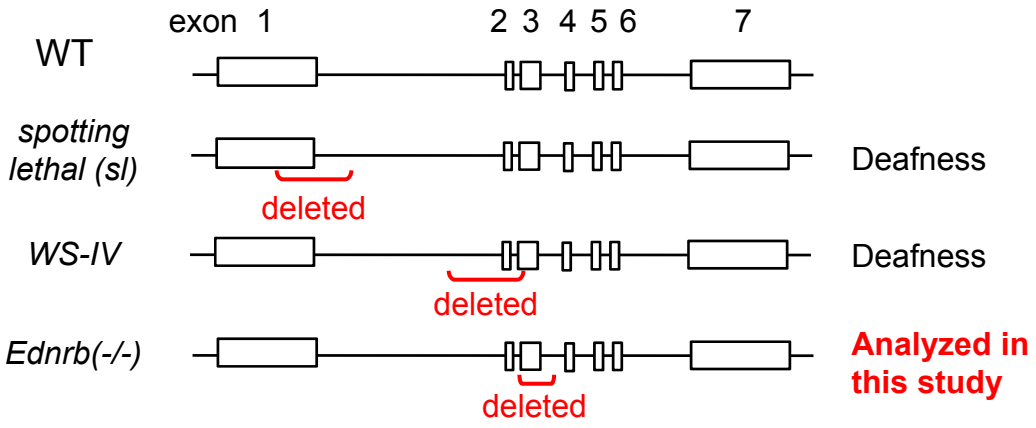

B

disorder	deafness	exon	amino acid change	nucleotide change	mutation	reference
Hirsch		1	(5'UTR)	G -> A	transversion hetero	4
Hirsch		1	G57S	GGT -> AGT	missense	5,6
WS		2	A183G	C -> G	missense	7
WS	deafness	2	G186R	GGA -> AGA	missense	8
WS	deafness	2	S196N	AGT -> AAT	missense	9
ABCD(WS)	bilateral deafness	**3**	R201(ter)	C -> T	nonsense	10,11
WS	deafness	**3**	R253(ter)	CGA -> TGA	nonsense	12
Hirsch		4	W275(ter)	G -> A	nonsense	13
Hirsch	deafness	4	W276C	G -> T	missense	14
Hirsch		4	(894ter)	insert T	flemeshift	13
Hirsch		4	S305N	G -> A	missense	15
Hirsch		5	R319W	GGG -> TGG	missense hetero	4
Hirsch		6	N378I	deletion A	frameshift	16
Hirsch		6	P383L	CCA -> CTA	missense hetero	4